Half-Metallic Exchange Bias Ferromagnetic/Antiferromagnetic Interfaces in Transition-Metal Chalcogenides

Kohji Nakamura,* Yoshinori Kato, Toru Akiyama, and Tomonori Ito
Department of Physics Engineering, Mie University, Tsu, Mie 514-8507, Japan

A. J. Freeman
Department of Physics and Astronomy, Northwestern University, Evanston, Illinois 60208, USA
(Received 1 September 2005; published 1 February 2006)

To investigate half-metallic exchange bias interfaces, magnetic structures at ferromagnetic (FM)/antiferromagnetic (AFM) interfaces in the zinc blende transition-metal chalcogenides, CrSe/MnSe and CrTe/MnTe with compensated and uncompensated AFM interfaces, were determined by the full-potential linearized augmented plane-wave method. With the uncompensated AFM interface, an antiparallel alignment of the Cr and Mn moments induces an excellent half-metallicity. More striking still, in the compensated AFM interface the Cr moments in the FM layer lie perpendicular to the Mn moments in the AFM layer but the Mn moments strongly cant to induce a net moment so as to retain the half-metallicity. These findings may offer a key ingredient for exchange biased spintronic devices with 100% spin polarization, having a unidirectional anisotropy to control and manipulate spins at the nanoscale.

DOI: 10.1103/PhysRevLett.96.047206 PACS numbers: 75.70.Cn, 73.20.−r, 71.20.Be

Exchange bias [1,2] induces a unidirectional shift of a hysteresis loop and an enhancement of coercivity and is a most important phenomenon that provides an ability to control and manipulate magnetic properties on the nanoscale. Indeed, for a first time, the exchange bias has been demonstrated to overcome the so-called ''superparamagnetic limit'' due to thermal fluctuations down to 4 nm diameter Co particles [3], and so is expected to surpass the Tbit/in^2 goal in the ultrahigh-density storage technology.

To date, many experimental and theoretical efforts have been performed to understand the exchange bias in metals, oxides, sulfides, fluorides, and nitrides. It is now agreed that an important role in accounting for this phenomenon is played by local magnetic structures at ferromagnetic (FM)/antiferromagnetic (AFM) interfaces, as well as by domain wall motions and defects in the FM and AFM volumes [2].

Most recently, strong attention has focused on the exchange bias in half-metallic systems such as ferromagnetic semiconductors in spintronic applications. Furdyna *et al.* [4] have recently observed an enhanced coercivity in dilute $Ga_{1-x}Mn_xAs$ and MnTe multilayers, suggesting proximity effects at the FM/AFM interfaces, and Eid *et al.* [5,6] have reported clear evidence of exchange bias in $Ga_{1-x}Mn_xAs$ grown on MnO. However, because of the complexity of the magnetic structures, e.g., the dilution and reactivity of Mn atoms at the interfaces, the reproducibility of the exchange bias in these materials is not yet established.

Unfortunately, half-metallicity in materials such as bulk Heuser compounds and zinc blende transition-metal pnictides is destroyed by the presence of interfaces with semiconductors [7–9], which reduces the spin polarization current. It may thus be expected that electronic structures of half-metallic FM materials, where one spin channel has a band gap at the Fermi level (E_F) while the other keeps a metallic character, would be strongly perturbed by contact with AFM materials.

In our search for half-metallic exchange bias systems, we have investigated for the first time FM/AFM zinc blende (ZB) transition-metal chalcogenides interfaces, CrSe/MnSe and CrTe/MnTe with both compensated and uncompensated AFM components, by means of the highly precise first principles full-potential linearized augmented plane-wave (FLAPW) method [10,11], including noncollinear magnetism [12,13]. With the uncompensated AFM interface, we find that an antiparallel alignment of the Cr and Mn moments is favored over the parallel one, which induces an excellent half-metallicity. By contrast, in the compensated AFM interface the Cr moments in the FM layer lie perpendicular to the Mn moments in the AFM layer, but the Mn moments strongly cant so as to induce a net moment opposite to the Cr direction, which tends to retain the half-metallic state. Thus, these interfaces offer a key ingredient as promising exchange bias candidates—most importantly, in having interfaces with 100% spin polarization and in inducing an anisotropy (having greater magnetization stability) to control and manipulate spins in the nanoscale, as required in high-performance nanospintronic applications.

Calculations were carried out based on the local spin density approximation with the von Barth–Hedin exchange correlation [14], in which the core states are treated fully relativistically and the valence states are treated scalar relativistically without the spin-orbit coupling (SOC). To treat the intra-atomic noncollinear magnetism, the electron density and the effective potential are treated with a 2×2 density matrix and the basis functions are specified with the spin-independent LAPW basis in order to avoid dis-

TABLE I. Total energy differences, $\Delta E = E_{\mathrm{AFM}} - E_{\mathrm{FM}}$ (in meV/f.u.), total magnetic moments, M (in μ_B/f.u.), and integrated moments in MT spheres of transition metals, m_{MT} (in μ_B), for zinc blende TM-As, TM-Se, and TM-Te compounds, where the TM are V, Cr, Mn, and Fe transition metals.

	TM-As (a_{GaAs})			TM-Se (a_{GaAs})			TM-Te (a_{InAs})		
TM	ΔE	M	m_{MT}	ΔE	M	m_{MT}	ΔE	M	m_{MT}
V	174	2.00	1.87	123	2.50	2.18	184	3.00	2.51
Cr	294	3.00	2.97	73	4.00	3.55	161	4.00	3.55
Mn	78	3.63	3.54	−319	0.00	3.96	−264	0.00	3.91
Fe	−213	0.00	2.75	−210	0.00	2.95			

continuity in augmentation of the basis functions at the muffin-tin (MT) radius [12,13]. The LAPW basis with a cutoff of $|\mathbf{k} + \mathbf{G}| < 3.9$ a.u.$^{-1}$ and MT sphere radii of 2.3 a.u. for the $3d$ transition metals (TM), and 2.0 a.u. for group-IV elements is used. Lattice harmonics with angular momenta up to $\ell = 8$ are employed to expand charge density, potential, and wave functions. At a later stage, we carried out the SOC calculations by using the second variation method [13], and found that the magnetic structures for both uncompensated and compensated AFM interfaces of CrSe/MnSe and CrTe/MnTe do not alter the scalar-relativistic results obtained [15].

We first discuss the calculated electronic and magnetic structures of the ZB transition-metal pnictides and chalcogenides given in Table I. The lattice constants of the TM-As and TM-Se, where the TM are V, Cr, Mn, and Fe, are assumed to match that of GaAs (5.65 Å), and for TM-Te, that of InAs (6.06 Å). Table I also gives calculated total energy differences between the collinear FM and AFM states, $\Delta E = E_{\mathrm{AFM}} - E_{\mathrm{FM}}$, the total magnetic moments, M, and the moments integrated in the MT spheres of the TM, m_{MT}. In all groups of interest here, the compounds having a small TM atomic number energetically favor the FM ground state, in which the VAs, CrAs, CrSe, CrTe, and VTe show half-metallic character with integer total moments. In contrast, on increasing the atomic number, the AFM state turns out to be favored over the FM state, in which MnSe and MnTe show insulating (semiconducting) states while FeAs and FeSe are now metallic. The trend in the results agrees with that in previous experimental and theoretical investigations [16–22].

Now, consider FM/AFM interfaces consisting of half-metallic FM, CrSe (CrTe), and insulating AFM, MnSe (MnTe). The insulating AFM material has an advantage in minimizing perturbations to the electronic states at E_{F} in the half-metallic FM layer in contact with the AFM material. Moreover, a combination of the CrSe and MnSe (CrTe and MnTe) satisfies a requirement to induce the exchange bias—namely, $T_{\mathrm{C}} > T_{\mathrm{N}}$ [23]. Also epitaxial growth of these bilayers may be feasible since the theoretically predicted equilibrium lattice constant of the CrSe (5.76 Å) is close to that of MnSe (5.72 Å) as is that for CrTe (6.11 Å) with that of MnTe (6.08 Å)—i.e., within 2% for both cases.

As a model of the FM/AFM interfaces, we employed six-atomic layers of CrSe (CrTe) and six-atomic layers of MnSe (MnSe) in (001) superlattice structures with the lattice constant of GaAs (5.65 Å) for CrSe/MnTe and that of InAs (6.06 Å) for CrTe/MnTe. With an uncompensated AFM interface (explained below), we confirmed that calculations modeled with ten-atomic-layer/ten-atomic-layer superlattices and including interface relaxation that expands the interlayer distances by 2% do not significantly change the results obtained.

We here assumed two AFM interfaces—uncompensated and compensated. The uncompensated interface has the AFM sheets perpendicular to the interface plane [Figs. 1(a) and 1(b)], in which the Mn moments on the interface plane point in the same orientation, while the compensated interface has the AFM sheets parallel to the interface [1(c) and 1(d)]. These alignments may be controlled by a tetragonal distortion induced in epitaxial growth [19]. Since the tetragonal distortion results in different exchange interactions parallel and perpendicular to the interface plane, which makes the exchange strength increase and decrease, the distortion with $c/a < 1$ may prefer the uncompensated AFM interface while that with $c/a > 1$, the compensated AFM interface.

For initial magnetic structures, we considered two plausible magnetic orderings at each interface: type I and II structures for the uncompensated AFM interface and

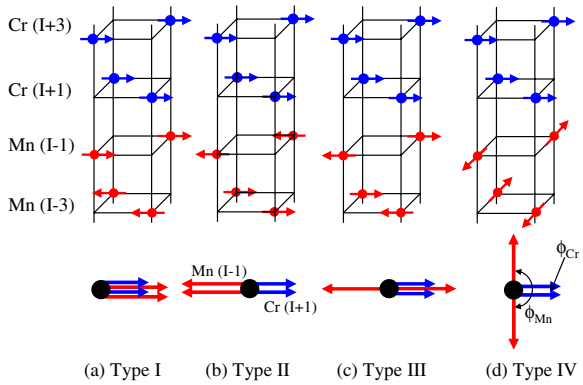

FIG. 1 (color online). Initial magnetic orderings, type I and II structures for an uncompensated AFM interface and type III and IV structures for a compensated AFM interface, where the As and Se are not shown. Arrows represent the average moment directions of Cr (blue) and Mn (red). The angles, $\phi_{\mathrm{Cr(Mn)}}$, between two Cr (Mn) in type IV structure are defined in (d).

TABLE II. Total energy differences, $\Delta E_{\mathrm{II,IV}}$ (in eV/a^2), and magnitude of magnetic moments in the MT sphere, m (in μ_B), for type II (uncompensated) and IV (compensated) structures of CrSe/MnSe and CrTe/MnTe. ϕ (in degrees) and m_{FM} (in μ_B) in type IV structure are the angle between two Cr (Mn) moment directions defined in Fig. 1 and the induced net moments along the average FM moment direction. The first column indicates layer positions (see Fig. 1).

		CrSe/MnSe				CrTe/MnTe			
		Type II	Type IV			Type II	Type IV		
$\Delta E_{\mathrm{II,IV}}$		−0.41	−0.08			−0.23	−0.03		
		m	m	ϕ	m_{FM}	m	m	ϕ	m_{FM}
$I+3$	Cr	3.53	3.54	3	3.54	3.53	3.54	4	3.54
$I+1$	Cr	3.56	3.40	0	3.40	3.38	3.44	0	3.44
$I-1$	Mn	−3.96	3.93	261	−2.56	−3.92	3.88	225	−1.49
$I-3$	Mn	3.95	3.95	103	2.44	3.89	3.89	139	1.37

type III and IV structures for the compensated AFM interface, as sketched in Fig. 1. In the uncompensated AFM interface, the Cr and Mn moments at the interface order parallel and antiparallel for the type I and II structures, respectively. The type III structure in the compensated AFM interface is collinear (where the Mn moments orient parallel and antiparallel to the Cr moments), while the type IV structure is noncollinear (where the Mn moment axis is perpendicular to the Cr direction).

Table II gives calculated total energy differences, $\Delta E_{\mathrm{II}}(= E_{\mathrm{II}} - E_{\mathrm{I}})$ and $\Delta E_{\mathrm{IV}}(= E_{\mathrm{IV}} - E_{\mathrm{III}})$. In the uncompensated AFM interface, we find that the type II structure is energetically favored over the type I by 0.41 and 0.23 eV/a^2 for CrSe/MnSe and CrTe/MnTe, respectively, and by 0.08 and 0.03 eV/a^2 for CrSe/MnSe and CrTe/MnTe in the compensated AFM interface type IV structure. Although the ground state is found to be the compensated AFM interface (type IV) for both CrSe/MnSe and CrTe/MnSe, the energy difference ($E_{\mathrm{IV}} - E_{\mathrm{III}}$) is rather small, −0.02 eV/a^2 for CrSe/MnSe and −0.04 eV/a^2 for CrTe/MnTe. This indicates, as mentioned above, that the tetragonal distortion in epitaxial growth will be important in controlling the magnetic structures.

Table II also summarizes the magnetic moments in the MT spheres along their average moment directions, m, the angles $\phi_{\mathrm{Cr(Mn)}}$ between the two Cr (Mn) moment directions illustrated in Fig. 1(d), and the induced net moments, m_{FM}, along the average FM moment direction. The Cr moments at the interfaces are $3.4\mu_B$ to $3.6\mu_B$, while the Mn moments are $3.9\mu_B$ to $4.0\mu_B$; they do not significantly change from the bulk values, $3.55\mu_B$ ($3.55\mu_B$) in CrSe (CrTe) and $3.96\mu_B$ ($3.91\mu_B$) in MnSe (MnTe). The induced Se and Te moments are also induced in an opposite orientation to the Cr direction in the FM layers with a small magnitude ($<0.1\mu_B$), while zero Se and Te moments in the AFM layers are observed due to the AFM Mn configuration surrounding these atoms. In the compensated AFM interface, the Mn moments strongly cant to induce large net moments opposite to the Cr direction.

As previously demonstrated [20], in bulk FM CrSe (CrTe), the Cr $3d\,t_{2g}$ states hybridize with nearest-neighbor Se (Te) p states, which induces a bonding-antibonding splitting, while the Cr $3d\,e_g$ states are unperturbed due to no p-d hybridization. The E_{F} is below the conduction band in the minority-spin state and the $3d$ carriers in the majority-spin states stabilize the FM structure through the double exchange mechanism.

When the CrSe (CrTe) is interfaced with the AFM MnSe (MnTe) as in a type I structure where the Cr and Mn moments at the interface couple in parallel, however, the number of electrons at the interface increases since Mn has one more electron than Cr, and so E_{F} will be shifted to higher energy if one assumes FM band structures; furthermore, this puts E_{F} into the minority-spin antibonding bands, causing the hole density to be small and the double

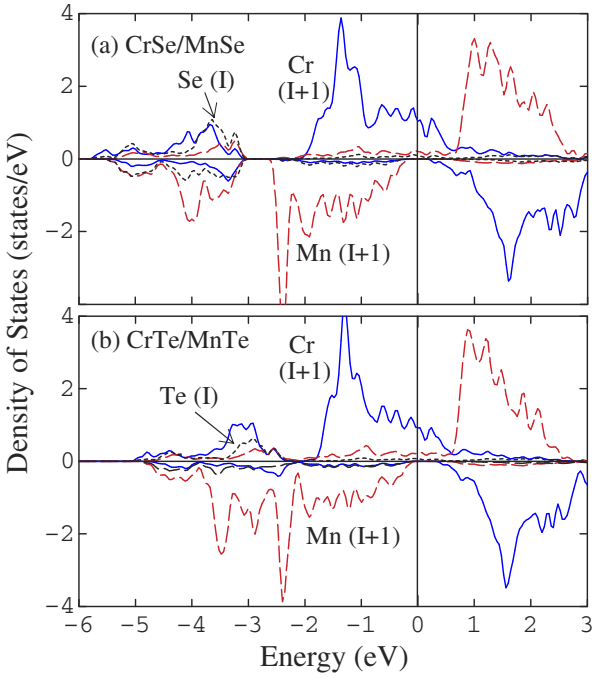

FIG. 2 (color online). Spin-projected density of states (DOS) for type II structure in the uncompensated AFM interface for (a) CrSe/MnSe and (b) CrTe/MnTe. Solid (blue) lines represent the DOS of Cr, dashed (red) lines are those of Mn, and dotted (black) lines, of Se or Te at the interface.

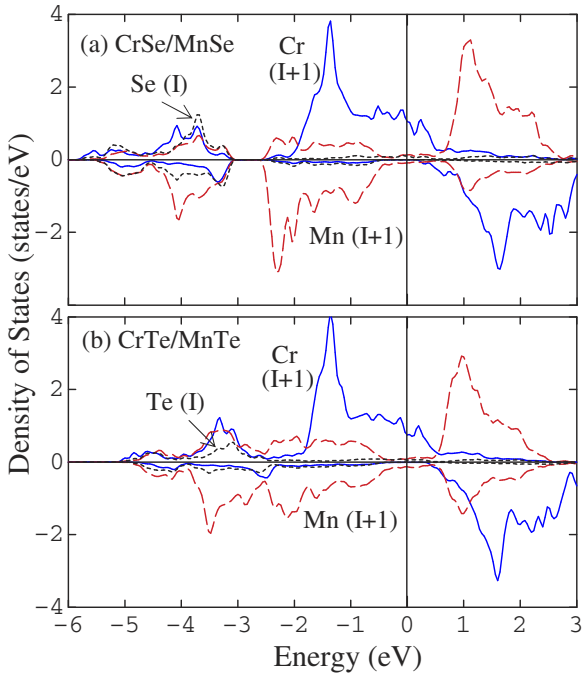

FIG. 3 (color online). Spin-projected density of states (DOS) along the average FM moment directions for type IV structure in the compensated AFM interface for (a) CrSe/MnSe and (b) CrTe/MnTe. Notations are the same as in Fig. 2.

exchange to be weak. Now, the superexchange interaction excites an antiparallel alignment of the Mn moments, where the minority-spin Mn^{2+} ($3d^5$) states hybridize with the majority-spin states on Cr sites through the interface Se (Te) p orbitals as seen in Fig. 2. In addition, the large intra-atomic exchange splitting in the Mn d bands ensures the band gap to be between the occupied Mn d and unoccupied Cr d bands in the minority-spin state. Thus, the half-metallicity is retained by the antiparallel alignment of the Cr and Mn moments, which leads to the stabilization of the half-metallic type II structure obtained.

In contrast, frustration at the compensated FM/AFM interface, where an equal number of positive and negative nearest-neighbor exchange interactions exist across the interface, leads to a perpendicular coupling [24]. However, the canting of the Mn moments is found to reduce the majority-spin DOS at E_F significantly, as seen in Fig. 3, so as to retain the half-metallic state at the FM/AFM interface. Furthermore, roughness such as steps, islands, or point defects at the compensated AFM interface would play a key role in the exchange bias [12,25]. Indeed, our FLAPW calculations for the (001) interface including a line step defect along [010] with a ten-atomic-layer superlattice [12] shows that a collinear antiparallel coupling of the Cr and Mn moments at the FM/AFM step with half-metallic character is highly favored over the parallel one with energy differences of 0.38 and 0.20 meV/a^2 for CrSe/MnSe and CrTe/MnTe, respectively. Thus, since the energy differences are sufficiently greater than the biquadratic exchange energies (ΔE_{IV} in Table II), the introduction of step defects in the flat interface induces a torque that causes the Cr moments to align antiparallel to the Mn moments, and leads to a unidirectional magnetic anisotropy of the exchange bias.

These results predict a class of promising half-metallic exchange bias candidates and invite experimental confirmation.

The work at Mie University was supported by a Grant-in-Aid for Scientific Research (Grants No. 16760024 and No. 16310081), and performed for computations at CRC and CITN, Mie University, and ISSP, University of Tokyo. The work at Northwestern University was supported by the National Science Foundation Grant No. DMR 0244711.

*Electronic address: kohji@phen.mie-u.ac.jp

[1] W. P. Meiklejohn and C. P. Bean, Phys. Rev. **102**, 1413 (1956); Phys. Rev. **105**, 904 (1957).
[2] J. Nogués and I. K. Schuller, J. Magn. Magn. Mater. **192**, 203 (1999), and references therein.
[3] V. Skumryev *et al.*, Nature (London) **423**, 850 (2003).
[4] J. K. Furdyna *et al.*, J. Appl. Phys. **91**, 7490 (2002).
[5] K. F. Eid *et al.*, Appl. Phys. Lett. **85**, 1556 (2004).
[6] K. F. Eid *et al.*, J. Appl. Phys. **97**, 10D304 (2005).
[7] G. A. de Wijs and R. A. de Groot, Phys. Rev. B **64**, 020402(R) (2001).
[8] S. Picozzi *et al.*, J. Appl. Phys. **94**, 4723 (2003).
[9] K. Nagao *et al.*, J. Appl. Phys. **95**, 6518 (2004).
[10] E. Wimmer *et al.*, Phys. Rev. B **24**, 864 (1981).
[11] M. Weinert *et al.*, Phys. Rev. B **26**, 4571 (1982).
[12] K. Nakamura *et al.*, Phys. Rev. B **65**, 012402 (2002).
[13] K. Nakamura *et al.*, Phys. Rev. B **67**, 014420 (2003).
[14] U. von Barth and L. Hedin, J. Phys. C **5**, 1629 (1972).
[15] Of course, we note the importance of the SOC that inherently causes an admixture of spin-up and spin-down electronic states, which might play an important role in spin-flip transitions in the spin polarized current.
[16] M. Yokoyama *et al.*, J. Appl. Phys. **97**, 10D317 (2005).
[17] P. Klosowski *et al.*, J. Appl. Phys. **70**, 6221 (1991).
[18] N. Samarth *et al.*, Phys. Rev. B **44**, R4701 (1991).
[19] T. M. Giebultowicz *et al.*, Phys. Rev. B **48**, 12 817 (1993).
[20] I. Galanakis and P. Mavropoulos, Phys. Rev. B **67**, 104417 (2003).
[21] B. Sanyal *et al.*, Phys. Rev. B **68**, 054417 (2003).
[22] S. H. Wei and A. Zunger, Phys. Rev. B **48**, 6111 (1993).
[23] K. Nakamura *et al.*, Phys. Rev. B **72**, 064449 (2005).
[24] N. C. Koon, Phys. Rev. Lett. **78**, 4865 (1997).
[25] T. C. Schulthess and W. H. Butler, Phys. Rev. Lett. **81**, 4516 (1998).